Iranian Journal of Astronomy and Astrophysics
Vol. 9, No. 1, Spring 2022

DOI:10.22128/ijaa.2022.633.1133

Iranian Journal of Astronomy and Astrophysics

Chromospheric Jets and Their Properties

Ehsan Tavabi[1] · Sima Zeighami*[2]

[1] Physics Department, Payame Noor University (PNU), 19395-3697-Tehran, I. R. of Iran;
email: e_tavabi@pnu.ac.ir
[2] Department of Physics, Tabriz Branch, Islamic Azad University, Tabriz, Iran;
*email: zeighami@iaut.ac.ir

Abstract. In this study, we review solar chromospheric jets and characteristics of them. The chromosphere and transition region are the interface between the solar photosphere and the corona, which plays a key role in the formation and acceleration of the solar wind. In recent years, scientists have made great efforts to understand the mechanism of energy transfer in the solar chromosphere and corona. The researchers suggest that the key to solving this problem may lie in understanding the nature of the small-scale transient events that are distributed across the surface of the Sun. Of these, solar spicules are the most prominent small-scale dynamical phenomena in the chromospheric regions that drive relatively cold material from the lower chromosphere to the corona. Spicules can heat the corona both by ejecting hot plasma and by energy transfer by magnetohydrodynamic (MHD) waves. These dynamical structures are formed when photospheric oscillations and convective flow along the magnetic field lines penetrate into the chromosphere.

Keywords: Chromosphere, Jets, Spicules, Oscillations, Plasma, Image Processing

1 The Solar Chromosphere

The coolest layer of the sun, which is called the thermal minimum region, includes 500 km above the photosphere, where the temperature reaches 4000 K. This region is cool enough to find water molecules and carbon monoxide. The presence of such molecules in this layer has been proven by spectroscopic methods and observation of the absorption line of these elements in the spectrum of sunlight. Above the region of the minimum thermal degree, there is a thin layer with a thickness of approximately 2000 km, which was discovered by spectroscopic methods and observation of spectral absorption lines. This layer is called chromosphere, which is derived from the word chroma (meaning color) [22]. The reason for choosing this name is that this layer is usually invisible due to the brightness of the photosphere. But, during a solar eclipse, when the moon covers the central disk of the sun, the red light of the chromosphere can be seen. This layer is mainly composed of hydrogen gas and sodium, calcium, magnesium and helium ions are also present in it. The chromosphere is visible like a colored arrow at the beginning and end of a total solar eclipse. The temperature in the chromosphere gradually rises with increasing height from the surface of the sun and reaches 100,000 K near the border of this layer. Figure 1, shows a representative model of the chromosphere [38].

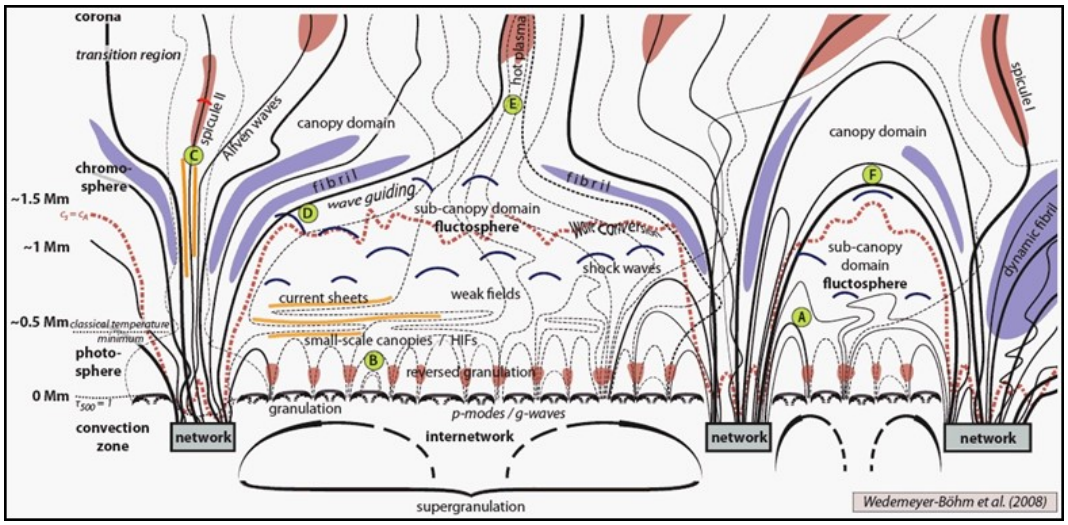

Figure 1: A representative model of the chromosphere [38].

2 Spicules

Spicules are jet-like structures that extend from the inside of the chromosphere to the corona in the form of gas eruptions (see Figure 1). The reason spicules appear in the corona in the form of moving spikes is that the density of the chromosphere material does not match the density of the material of the sun's corona. Spicules play an important role in the mass balance of the solar corona. The luminosity of spicules changes with changes in temperature and height, and they can travel several thousand kilometers to reach the peak point, and after reaching the maximum height, two situations occur: 1- with a speed almost equal to the speed of going down, that is, they fall into the chromosphere 2- in the transition zone fades from view and transports matter to the Sun's corona [39,41]. In this way, spicules can compensate for the mass lost by the sun's corona due to the solar wind and establish mass balance. If the spicules are slightly longer and more vertical in the cavities of the corona and slightly more in the poles than in lower latitudes. The energy carried by the spicules is transferred to the outside in the form of waves and oscillations that propagate in them. In recent years, spicules have been widely studied, but a complete description of the formation process and dynamics of spicules has not been obtained so far. [5] Identified two types of spicules. The first type are spicules with typical lifetimes of 150-400 s with upward and downward movements on parabolic trajectories with maximum upward velocities of 40-15 kms^{-1} and often with accelerations between 50 and 400 kms^{-2} [4,18,45]. [4,6,8] proposed that dynamic fibrils are driven by magnetohydrodynamic shocks that result from currents and waves that leak from the photosphere to the chromosphere along magnetic field lines [8,4,6]. The behavior of type I spicules when observed in H is similar to active region , dynamic fibrils and some are similar to motels in the quiet Sun [8, 4, 21, 20]. These authors found a linear correlation between deceleration and maximum velocity observed in fibrils and mattes. MHD simulations in 2D and 3D showed the observed parabolic trajectories, decelerations, and very good maximum velocities [8,4]. The lifetime of these jets depends on the inclination of the magnetic field in the photosphere and lower chromosphere. The tilting of the field reduces the acoustic cut-off frequency and allows the photospheric wave spectrum with a dominant five-minute period of P-mode [11,13]. Regions where the field

is more vertical are governed by the three-minute chromospheric acoustic cutoff frequency. Type II spicules have only upward motions, shorter lifetimes, and higher velocities. [14] determined a typical speed of 110-30 kms^{-1} and a lifetime of 50-150 seconds. Type II spicules are mainly present in both quiet sun and coronal holes; but type I spicules dominate in active regions [5,14]. Figure 5 obtained using the FLCT algorithm for showing the 2D velocity maps from successive frames with a corresponding remarkable structure shown by the red arrow over a larger FOV shown in negative at the center [28].

3 Image processing

Since space observations are far from disturbing effects by the earth's atmosphere, they are superior to ground data, but these data are subject to other effects that are often caused by telescope slippage and the failure of its motors to follow properly. These effects in the case of telescopes can be eliminated by programs. These softwares calibrate the images taken from the telescope. [33] used 2D Wiener filter, which minimizes the overall mean square error in the process of filtering and noise smoothing. The base of this algorithm is the application of an operator pixelwise adaptive method which computes the maximum convexities in several directions around each pixel and it is shown to be efficient also for pattern recognition. In this method, a derivative of a 2D Gaussian function as a convolution enhances the visibility of thin structures, equivalent to a 2D Fourier filtering and it is very useful for evaluating thin structures as solar spicules. For increasing the visibility and contrast of thin solar structures a multidirectional (8, 16, ...) maximum gradient operator OMC (Operator Maximum Convexities) introduced by [12] and called Madmax. This operator works successfully for improving the visibility of solar spicules. [33] used this algorithm for improving the visibility of images, to trace the bright hair-like features of solar observations. Figure 2 presents inverted and calibrated image using the Hinode fg_preb SSW program, and the OMC (Madmax) reconstructed images in 8 and in 16 directions.

4 Physical characteristics of spicules

The upper parts of the spicules become progressively thinner and fade, making it very difficult to measure their length. Usually, instead of height, it is defined a height range. This altitude extends from 6500 to 13000 km. The very long spicules are known as macrospicules and can reach up to 40 Mm in the polar regions of the Sun [7,3,31]. The diameter of the spicules is about 100 to 2000 km. In spectral studies in different filters, the Ca II H spectral line with a wavelength of 5396.8 Å appears wider than the spectral region of H with a wavelength of 6562.8 Å. The lifetime of spicules is about 5 to 15 seconds and sometimes it happens as repeated phenomena with an interval of 3 to 5 minutes to 10 to 15 minutes. Spicules are approximately 100 times denser than their surroundings, which have a density of about 10^9 electrons per cm^3. The electron density is about 10^{11} electrons per cm3 or the mass density is $3\times\ 10^{-13}$ gcm^{-3}. Tilt of spicules has been reported to be less than 20 degrees, which is different for different latitudes of the sun, so that it reaches less than 10 degrees in the polar regions. spicules can be observed in addition to H and H (3968.5 Å) and K (3933.7 Å) wavelengths corresponding to doubly ionized calcium, in addition to neutral helium spectral lines with wavelengths of 10380 Å and 5880 Å in Ultraviolet and far ultraviolet wavelengths are also visible [44,37,21]. Doppler transmission measurements in the spectrum of spicules have obtained velocities of the order of 25 to 30 kms^{-1} for the ascent of spicules. These speeds are not only related to their up and down movements and may also

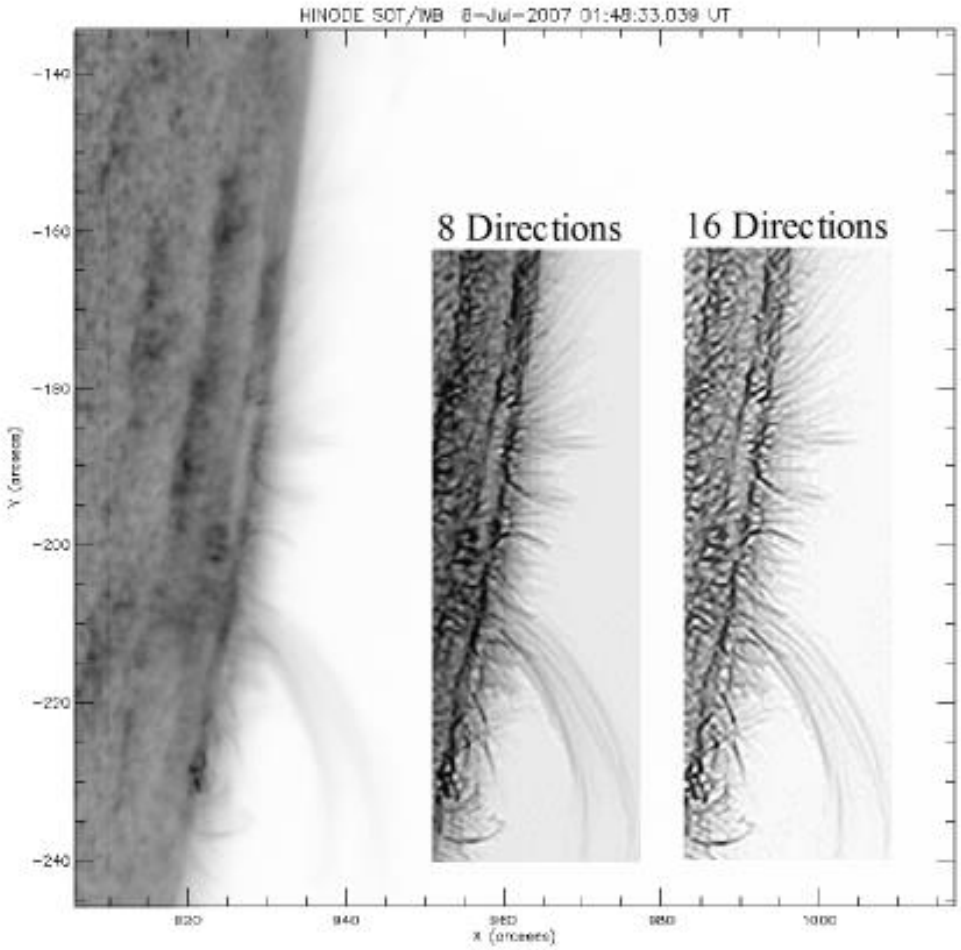

Figure 2: From left to right, inverted and calibrated image using the Hinode fg_preb SSW program, and the OMC (Madmax) reconstructed images in 8 and in 16 directions [33].

result from the transverse movements of the axis of the spicules, such transverse movements in the axis of the spicules result from the propagation of waves in them. Spicules cover about 0.1 of the Sun's surface, and at any moment, more than 300,000 spicules can be seen in the solar chromosphere. In addition to transverse oscillatory movements, some spectral studies of spicules show rotation around their axis. Most of the time, the speed value remains constant along the spicules and does not show a large decrease with the increase in height. This speed is related to the spectral measurements of the plasma speed inside the spicules, but the speed of the Alfven wave and other sound waves also exist, which in turn is very different from this value [40]. [29] obtained phase speeds of spicules as 50-450 kms^{-1} for quiet Sun, and 50550 kms^{-1} for active Sun. They also found strong evidence for upwardly propagating waves with high coherency in three datasets. [28] reported several Hinode/SOT long series observations in Ca H line and studied dynamical behavior of spicules. They Computed 2D velocity map by using FFTs and cross-correlation method, and use a 2nd-order accurate Taylor expansion

on highly processed images to locate the peak of the cross-correlation function to sub-pixel accuracy and found that almost a large percent of solar coronal hole spicules show surge-like behavior in support of twisty multi-components spicules (see figures 5-7).

5 Oscillations in spicules

Fluctuations in the spicules of solar limb can be observed in both visible and spectral ways [27,42]. Visible observations show fluctuations in the intensity of spicules and apparent movements of their axis. Such observations have become more important after the launch of the Hinode spacecraft [29, 28] . The solar optical telescope mounted on this spacecraft has made it possible to observe these fluctuations with a degree of spatial and temporal resolution [29,28,35]. Oscillations and transverse displacement of spicules axis can be interpreted due to the existence of transverse waves along their axis. The two types of waves that are responsible for these fluctuations are magneto-hydrodynamic waves (see Figure 8) and Alfven waves. If we consider spicules as plasma currents that exit in the direction of magnetic flux tubes, we can consider transverse kink and sausage waves as the cause of oscillation in spicules.If spicules are not stable waveguides for propagating tube waves, Alfven waves will cause oscillations in spicules. Spectroscopic studies provide valuable information about spicules through changes in the profile of spectral lines and the changes in Doppler shift in these lines, the line-of-sight velocity and its changes with time and altitude from the sun's surface. Through the broadening of spectral lines, it is possible to measure the non-thermal rotational speeds that lead to the indirect observation of torsional Alfven waves. [16] was the first to show three-minute oscillations inside the spicules through the Doppler shift of the spectral lines, and later [19] further investigated the spectral lines of hydrogen, and others' results confirmed the rotational motion inside the spicules. Because the spectral lines showed a skewness with a separation of less than 450 km and this skewness was also seen at high altitude where spicules overlap less. This curve showed that there is a rotation speed of 20 to 30 kms^{-1} inside the spicule [17,28]. Some observations suggest that solar spicules show small amplitude and high frequency oscillations of magneto-acoustic waves, which arise from photospheric granular forcing. [1] studied the temporal behavior of intensity fluctuations of spicules and macro-spicules observed at the solar limb by TRACE (transition region and coronal explorer) EUV telescope in the 1600 Å channel. Using wavelet analysis technique, they got evidence of spicule oscillations with periods of about 210-260 s with a typical lifetime of 10 min. [2] applied the method of MHD seismology to determine the period of kink waves, by purposing the oscillations of a magnetic cylinder embedded in a field-free environment. They found that oscillatory period in terms of some equilibrium parameters are provided to allow a comparison between theoretical results and observations. [9,10] identified spicules in the chromospheric and transition regions that were amplified by high-frequency transverse oscillations ($\geqslant$ 0.02 Hz). They proposed that such oscillations are Alfven waves traveling upward along the spicules with phase velocities of 50-150 kms^{-1}.

In order to show the origin and possibly explain spicule quasi-periodic recurrences produced by overlapping effects, [35] presented a simulation model assuming quasi-random positions of spicules, with different physical properties such as height, lifetime and tilt angle. They analyzed results of simulations made with three different spatial resolutions and also for different number density of spicules, using wavelet method, from the Transition Region and Coronal Explorer (TRACE) filtergrams taken at 1600 Å, the Solar Optical Telescope (SOT) of Hinode taken in the Ca II H-line and the H line. Their results suggested that when the spatial resolution is not enough to resolve individual components of spicules, overlapping is present. Figure 9 shows their results of simulations, and corresponding wavelet powers for

the integrated intensity fluctuation. By comparing observations and simulations, [15] suggested that the transverse displacement of the spicules can be explained by the propagation of Alfven waves, which are excited by the granular motions or general oscillating patterns of the Sun. They measured the phase velocity of oscillations in the coronal cavity, quiescent Sun, and active region perturbations (transverse continuum propagation associated with spicules) by cross-correlation of space-time curves at different heights. They measured the phase velocity of active regions perturbations at about 600 kms^{-1} observed by satellite (SDO/AIA) at line 171Å. They determined the period of oscillations in active region as 100-400 s. [14] studied intensity fluctuations with Hinode / SOT observations in Ca II H and analyzed the intensity spectrum of fluctuations according to the relative phase difference, time delay, and lateral correlation [25]. They found that the non-magnetic intensity fluctuations show a strong oscillatory power in the 3-7 mHz band, which is concentrated at 4.5 mHz, but this power weakens with the increase of the magnetic field. They found that the maximum coherence was in the range of 4-7 mHz. [13] investigated the oscillations in the active region loops simultaneously with two Hinode/EIS and SDO/AIA telescopes and using the wavelet method identified two situations where short-term oscillations, less than 1 minute, up to 3 minutes, and had long periods 9 min. They revealed upward perturbations propagating with an apparent velocity of 83.5 ± 1.8 to 100.5 ± 4.2 in lines 171Å and 193Å. [23] revealed oscillations that sometimes appeared to propagate along the spicules at speeds between 18-108kms^{-1}. They can be interpreted as Alfven waves. [24] Studied dynamical behavior of spicules by unprecedented high resolution Ca II H line emission time series, and showed that most of spicules have multiple structures, similarly to the doublet spicules, and they show impressive transverse periodic fluctuations which were interpreted as upward kink or Alfven waves with typical periods of the apparent oscillation being around 120 s, (see Figure 10). [30] applied Hough transform to the resulting images for making a statistical analysis of spicule orientations in different regions around the solar limb, from the pole to the equator. Spicules are visible in a radial direction in the polar regions with a tilt angle (less than 200). The tilt angle is even reduced to 10 degrees inside the coronal hole with open magnetic field lines and at the lower latitude the tilt angle reaches values in excess of 50 degree.

[26] investigated transverse oscillatory motions and recurrence behavior in the chromospheric jets observed by Hinode/SOT, and X-ray jets as shown in Figure 12 . They observed A jet like bundle observed at the limb in Ca II H line appears to show a magnetic topology that is similar to X-ray jets (as Eiffel tower shape). The appearance of such magnetic topology is usually assumed to be caused by magnetic reconnection near a null point. They studied the dynamical behavior of an incompressible magnetic X-point occurring during the magnetic reconnection in the jet formation region. The viscous effect is specially considered in the closed line-tied magnetic X-shape nulls. They performed the MHD numerical simulation in 2-D by solving the visco-resistive MHD equations with the tracing of velocity and magnetic field. They presented a qualitative agreement with Hinode observations for the oscillatory and non-oscillatory behaviors of the observed solar jets in both the chromosphere and the corona. Their results suggested that the viscous effect contributes to the excitation of the magnetic reconnection by generating oscillations. [34] investigated the counterpart of limb spicules foot-points on the disk, and this re-examination indicated that the interpretation of transverse motion of off-limb spicules could directly be related to rotational motion at the feet of disk spicules. Related bright elements move and vary in brightness on the timescales of chromospheric oscillations. The motions are similar to random displacements of the bright elements along the network boundaries with amplitudes of about 200 to 400 km, with evidence of spinning or vortex motion. They found a clear evidence and in several cases for splitting process and suggesting a formation mechanism for doublet (or

multi-component) spicules. A general inter chromospheric network velocity pattern with twists existing before the emergence and eruption of spicules seems to be required. They presented a helical kink mode propagation consistent with the new evidence of spicule multiple structure and provides an explanation for the origin of the Alfvenic wave propagation along the spicules(see Figure 14). Because the spinning spicules remains unclear from disk Dopplergram observations, they used a 3D time slice column diagrams (2D in x and y and time in z being the 3d dimension) by consecutive partly transparent slices put in perspective to show the rotational behavior at the chromospheric rosettes, and provide a wealth of information on spinning motion, helical wave propagation and splitting. [25] analyzed observations of a solar quiet region obtained using Hinode Solar Optical telescope (SOT) in Ca II H line, to study off-limb and on disk spicules and counterpart of limb spicule on the disk. In this study, 3 minute oscillations were well observed out of the limb and on the disk bright regions. The relationship between these features has been looked using power spectra distribution and show similar peaks, meaning similar periodicities. They detected both 3 and 5 minutes oscillations in bright points and mottles with dominate peaks (see Figure 15). [43] studied spectral images recorded by the IRIS Space Telescope (Interface Region Imaging Spectrograph) on August 17th, 2014 (Figure 16). They investigated the oscillatory properties of the solar spicules. They calculated Doppler velocity displacements up to a height of 4200 km from the edge of the sun by Gaussian fitting of the intensity profiles at the Si IV wavelength (Figure 17). They obtained average range of Doppler velocity from 12 to 15 kms^{-1} (blue shift) to 10 to 15 kms^{-1} (red shift). Their results of wavelet analysis revealed quasi-periodic fluctuations with dominant periods of 3, 5 and 8 minutes (Figure 18). According to their results, they suggested that the main contribution of the Doppler shift fluctuations, which were observed transversely perpendicular to the axis of the spicules, is caused by kink and Alfven waves. These waves can play an important role in heating the corona up to two million Kelvin. [27] studied in details the position of the EEs, and showed the very rapid blue- and co-temporal redshifts, in the C II and Mg II k raster Dopplergrams in the velocity space, that described in the literature as Alfvenic waves propagation. [32] studied motions and oscillations in the solar chromosphere and analyzed Doppler shifts observed off- limb with the Interface Region Imaging Spectrograph (IRIS). They found large transverse oscillations (see Figure 19). They determined for the first time waves with a short period of order of 100 sec and less and transverse amplitudes of order of $\pm$ 20 to 30 kms^{-1} . [36] investigated Explosive Events (EEs) in the off-limb solar atmosphere, with simultaneous observations from the Si IV, Mg II k, and slit-jaw images (SJI) of IRIS. They suggested that the fluctuations in the explosive events (EEs) illustrate swaying and rotational motions (see Figure 20).

6 Summery

Highly dynamic chromosphere can induce magnetohydrodynamics (MHD) waves, which are capable of propagating toward the chromosphere and solar corona. In order to know the physical structure of the layering of the sun's atmosphere, how heat and matter are transferred to the surface of the sun, and the effects of such transfers, it is necessary to study spicules. According to the observation of the sun's atmosphere in space stations and telescopes that are available today, it is possible to study these structures. The dynamic mechanism of the spicules of the chromosphere and the transition region can be revealed through these images with a high spatial resolution. Spicules are analyzes in either spectral or imaging method. In this research, we review physical characteristic of chromospheric jets and the propagation of wave oscillations from the chromosphere to the upper layers of the solar

atmosphere. The importance of chromosphere is that this layer is the main place of energy transfer from the solar surface to the very hot corona of the sun. The observations of spicules present the high dynamic and complex nature of the solar chromosphere and also illustrate that the dynamics of the chromosphere is important in the transportation of mass and energy from chromosphere to the corona.

References

[1] Ajabshirizade, A., Tavabi, E., & Koutchmy, S. 2008, New Astronomy, 13, 93.

[2] Ajabshirizade, A., Tavabi, E., & Koutchmy, S. 2009, Ap&SS, 319, 31.

[3] Dere, K. P., Baratoe, J. D. F., & Brueckner, G. E. 1983, ApJ, 267, 65.

[4] De Pontieu, B., Hansteen, V. H., Rouppe van der Voort, L., van Noort, M., & Carlsson, M. 2007, ASP, 368, 65.

[5] De Pontieu, B., McIntosh, S., Hansteen, V. H., Carlsson, M., & *et al.* 2007, Publ. Astron. Soc. Jap. 59, 655.

[6] De pontieu, B., Erdelyi, R., & James, S. 2004, Nature, 536, 430.

[7] Filippov, B., & Koutchmy, S. 2000, Solar Phys. 196, 311.

[8] Hansteen, V. H., DePontieu, B., Rouppe van derVoort, L., vanNoort, M., & Carlsson, M. 2006, ApJ, 647L, 73H.

[9] He, J. S., Tu, C. Y., Marsch, E., Guo, L. J., Yao, S., & Tian, H. 2009, A&A, 497, 525.

[10] He, J., Marsch, E., Tu, C., & Tian, H. 2009, ApJ, 705, 217.

[11] Jefferies, S. M., Mcintosh, S. W., Armstrong, J. D., Bogdan, T. J., Cacciani, A., & Fleck, B. 2006, ApJ, 648, L151.

[12] Koutchmy, O., & Koutchmy, S. 1989, Optimum filter and frame integration application to granulation pictures, in: von der Luhe, O. (Ed.), Proceedings of 10th Sacramento Peak Summer Workshop, High Spatial Resolution Solar Observations. National Solar Observatory, Sunspot, 217.

[13] Krishna Prasad, S., Banerjee, D., & Jagdev S. 2012, Solar Phys. 281, 67.

[14] Lawrence, J. K., & Cadavid, A. C. 2012, Solar Phys., 280, 125.

[15] McIntosh, S. W., De Pontieu, B., Carlsson, M., Hansteen, V., Boerner, P., & Goossens, M. 2011, Nature, 475, 477.

[16] Nikolsky, G. M., & Platova, R. 1971, Sol. Phys. 18, 403.

[17] Noyes, R. W. 1967, Observational Studies of Velocity Fields in the Solar Photosphere and Chromosphere. Aerodynamics Phenomena in Stellar Atmosphere, I.A.U. Symp. 28., 293.

[18] Pereira, T. M. D., De Pontieu, B., & Carlsson, M. 2012, ApJ, 759, 18.

[19] Pasachof, J. M., Noyes, R. W., & Beckers, J. M. 1968, Solar Phys., 5, 131.

[20] Rouppe van der Voort, L., De Pontieu, B., Hansteen, V., Carlsson, M., & van Noort, M. 2007, ApJ, 660, L169.

[21] Suematsu, Y., Wang, H., & Zirin, H. 1995, ApJ, 450, 411.

[22] Stix, M. The Sun. s.l.: Springer, 2002.

[23] Sekse, D. H., Rouppe van der Voort, L., De Pontieu, B., & Scullion, E. 2013, 44, 11.

[24] Tavabi, E., Koutchmy, S., & Ajabshirizadeh, A. 2011, New Astronomy, 16, 296.

[25] Tavabi, E. 2014, Ap&SSL, 352, 43.

[26] Tavabi, E., & Koutchmy, S. 2014, Ap&SSL, 352, 7.

[27] Tavabi, E., Koutchmy, S., & Golub, L. 2015, SoPh., 290.

[28] Tavabi, E., Koutchmy, S., Ajabshirizadeh, A., Ahangarzadeh Maralani, A. R., & Zeighami, S. 2015, A&A, 573, 7.

[29] Tavabi, E., Ajabshirizadeh, A., Ahangarzadeh Maralani, A. R., & Zeighami, S. 2015, J. A&A, 36, 307.

[30] Tavabi, E. 2012, J. Mod. Phys., 3, 1791.

[31] Tavabi, E. 2018, MNRAS., 476, 868.

[32] Tavabi, E., & Koutchmy, S. 2019, ApJ., 883, 41T.

[33] Tavabi, E., Koutchmy, S., & Ajabshirizadeh, A. 2013, Solar Phys. 283, 187.

[34] Tavabi, E. 2014, Ap&SS, 350, 489.

[35] Tavabi, E., Koutchmy, S., & Ajabshirizadeh, A. 2011, Advances in Space Research, 47, 2019.

[36] Tavabi, E., Zeighami, S., & Heydari, M. 2022, Solar Physics, 297, 1.

[37] Wilhelm, K. 2000, A&A, 360, 351.

[38] Wedemeyer-Bohm, S., Lagg, A., & Nordlund, A. 2009, Space Sci. Rev. 144, 317.

[39] Xia, L. D., Popescu, M. D., & Doyle, J. G. 2005, A&A, 438, 1115.

[40] Zaqarashvili, T. V., & Erdelyi, R. 2009, Space Sci. Rev., 149, 355.

[41] Zeighami, S., Ahangarzadeh Maralani, A. R., Tavabi, E., & Ajabshirizadeh, A. 2016, Sol. Phys. 291, 847.

[42] Zeighami, S., Tavabi, E., & Amirkhanlou, E., 2020, J. A&A, 41, 18Z.

[43] Zeighami, S., & Tavabi, E. 2021, Journal of the Earth and Space Physics.

[44] Zeighami, S., & Tavabi, E. 2021, IJAA.

[45] Zeighami, S., Tavabi, E., & Ajabshirizadeh, A. 2022, Journal of the Earth and Space Physics.

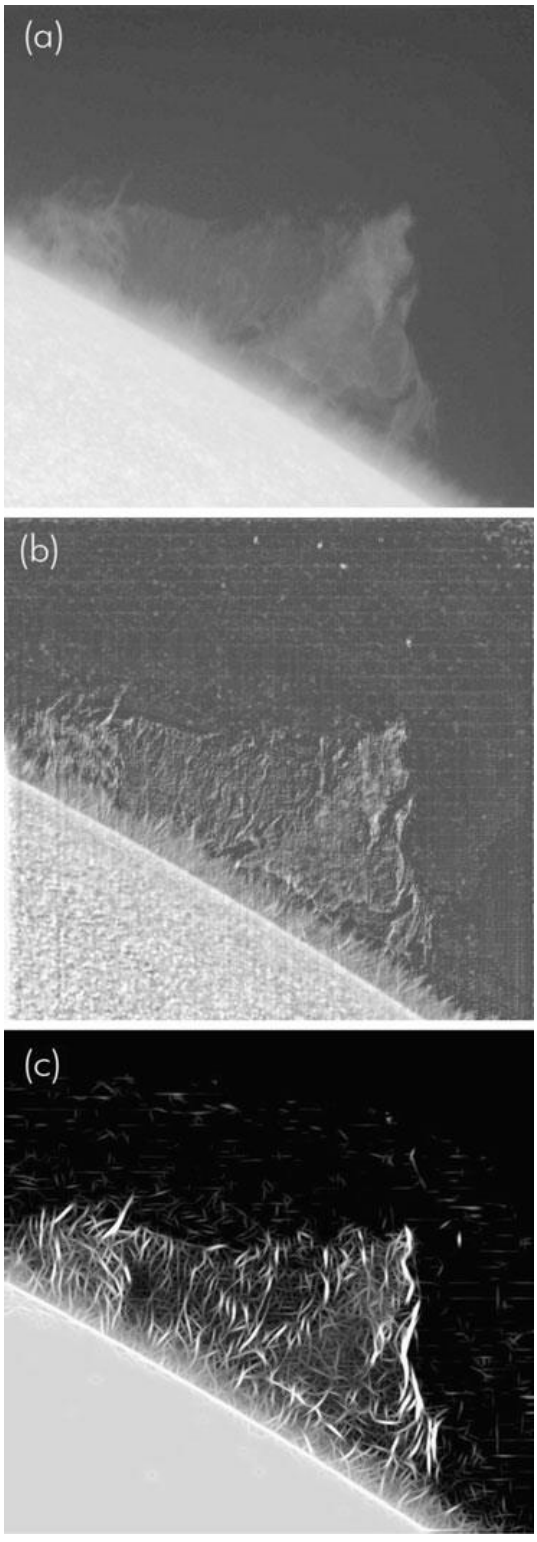

Figure 3: (a) A Ca II H line image of a prominence on 22 June 2010 observed with Hinode/SOT. The image has been calibrated (level_1) and then contrast enhanced. (b, c) The reconstructed images using the OMC filter with second derivatives in 8 (b) and 16 (c) directions, respectively. The horizontal and vertical lines seen in the background of panel (b) are due to row- and column-blocks of the CCD, which were eliminated in panel (c) by using, additionally, the 2-D Morlet wavelet filtering [33].

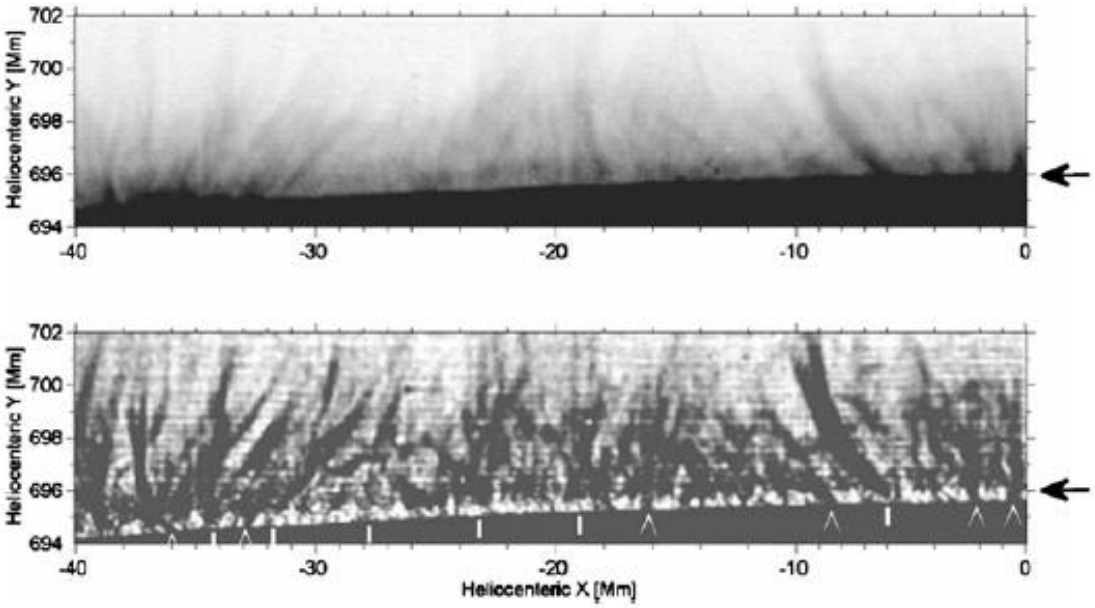

Figure 4: Ca II H (SOT- Hinode) limb original reconstructed negative, and the corresponding OMC (Madmax) filtergram obtained by superposing and aligning individual frames taken during 5 min at an 8 sec cadence. Arrows point to the same location right above the limb where the image processing performs very efficiently [33].

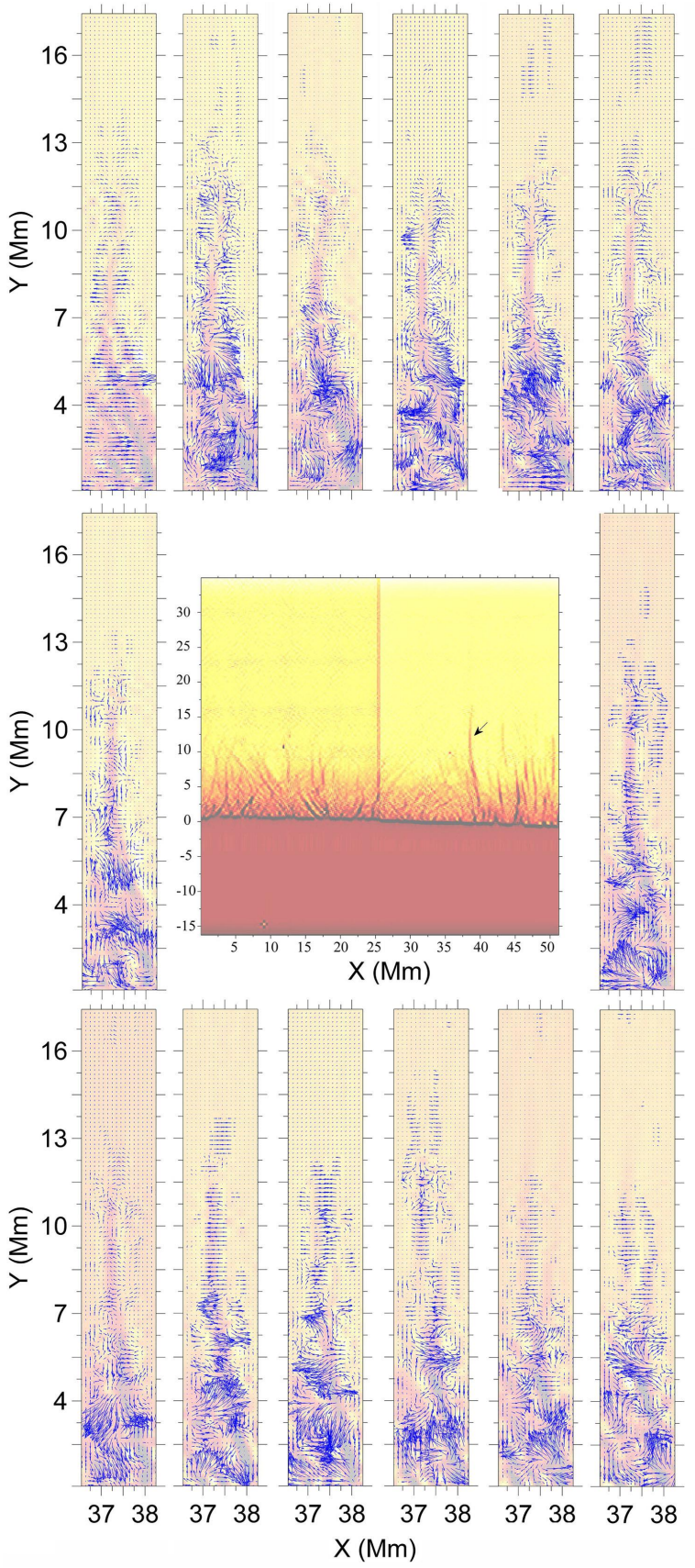

Figure 5: Example obtained using the FLCT algorithm for showing the 2D velocity maps from successive frames with a corresponding remarkable structure shown by the red arrow over a larger FOV shown in negative at the center [28].

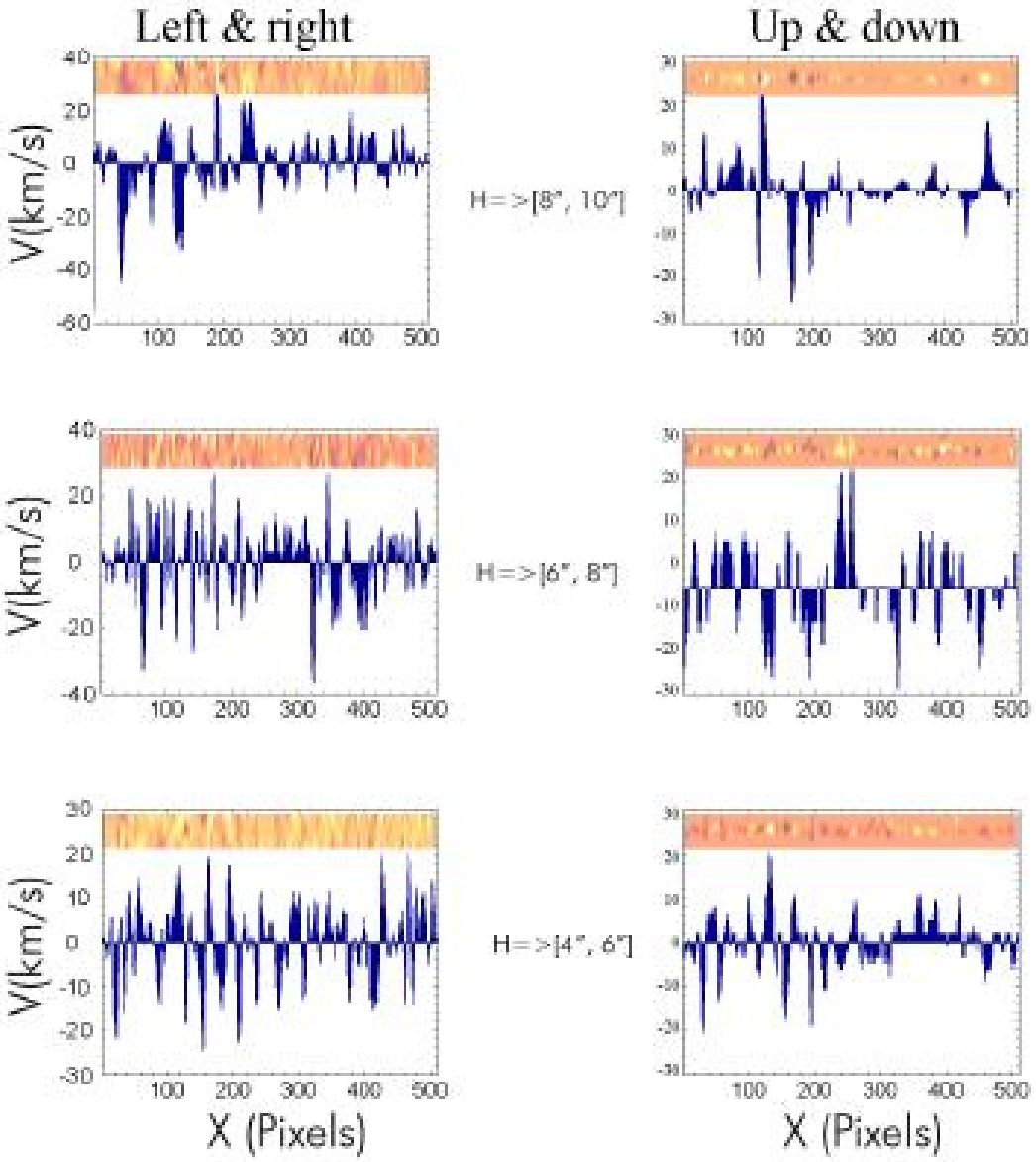

Figure 6: Distribution of horizontal and vertical proper motion velocities for different layers or slices above the limb as given by the height H in arcsec above the surface (limb) as observed on 17 June 2011. The orange band at the top shows the area selected at different heights, and the plots show the dispersion around the mean values [28].

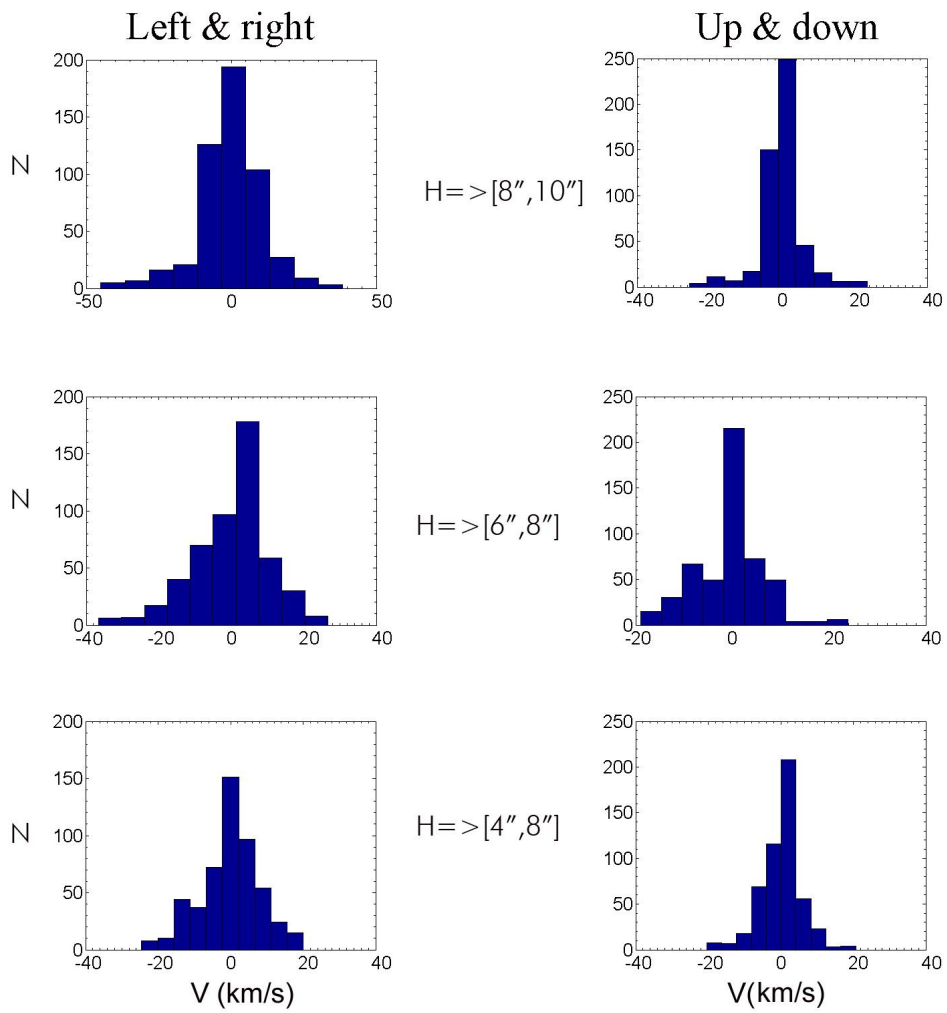

Figure 7: Histograms for swaying and up and down motions for different heights observed on 17 June 2011 [28].

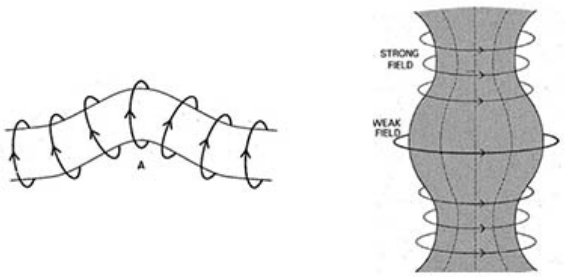

Figure 8: kink and sausage mode.

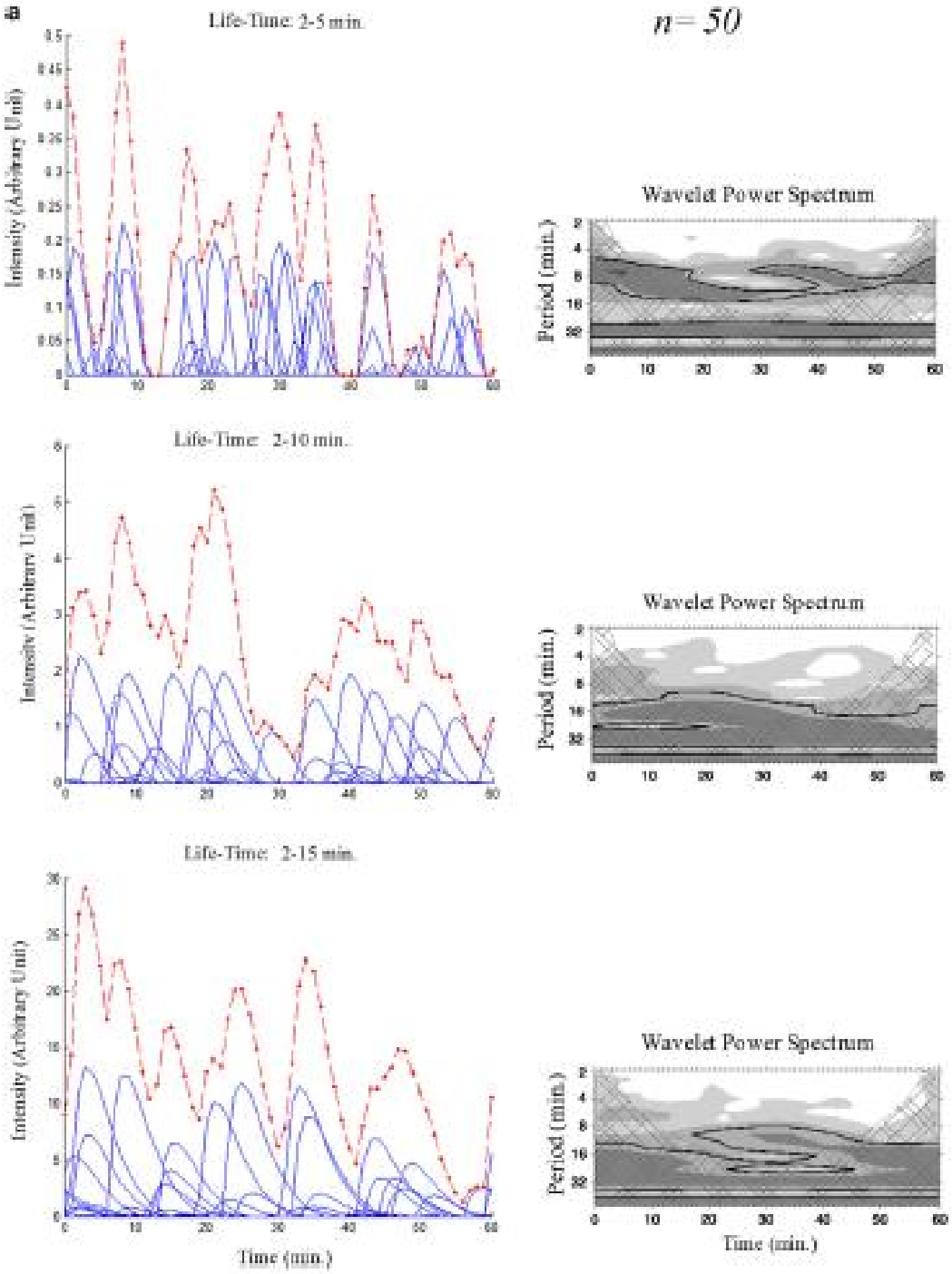

Figure 9: Left frames show the results of simulations, and the right plots show the corresponding wavelet powers for the integrated intensity fluctuation [35].

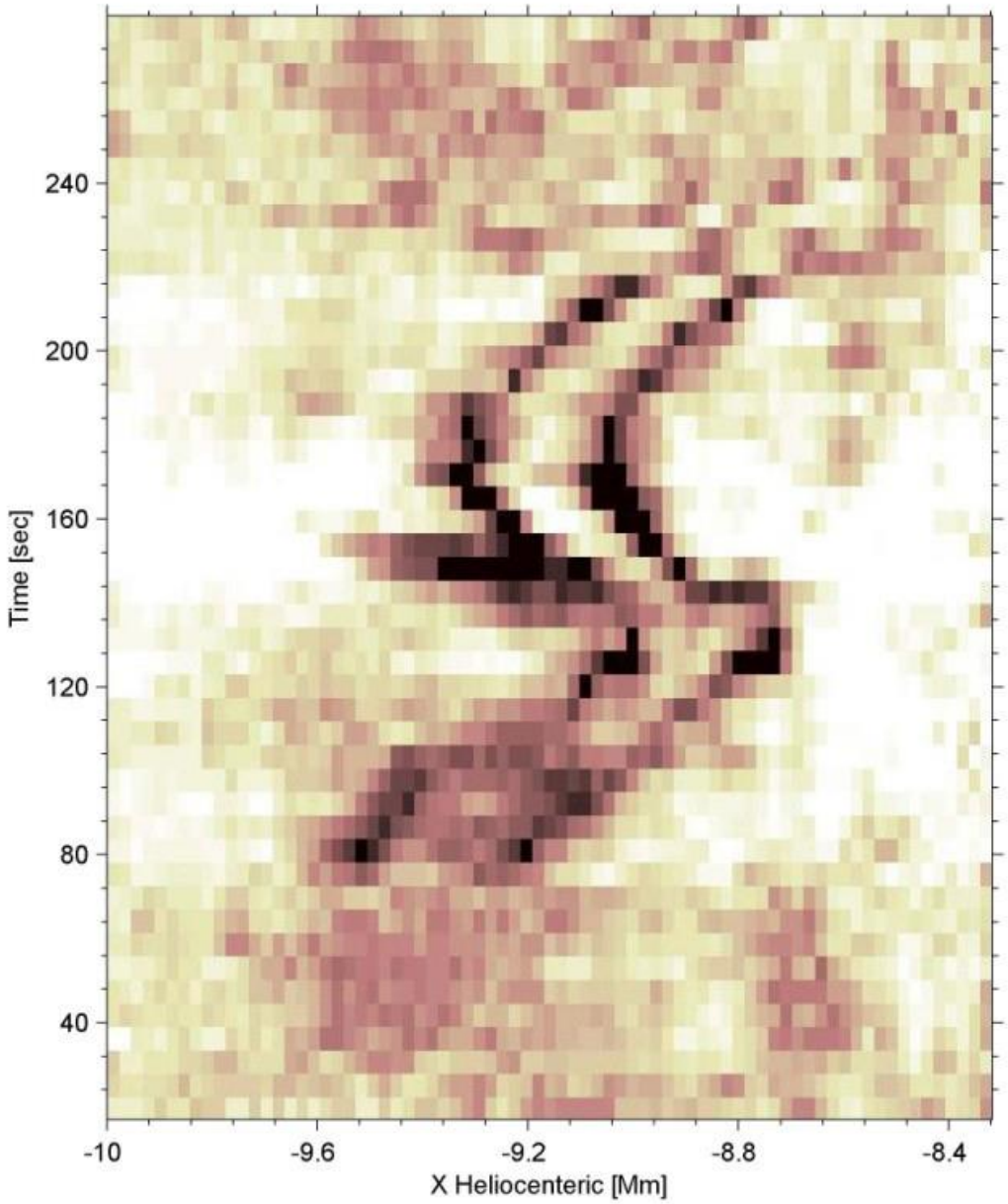

Figure 10: Time slice image in negative from the Ca II H line SOT observations from Hinode. The x axis corresponds to heliocentric coordinates in Mm. The wave like pattern of a doublet spicule is dramatically illustrated [24].

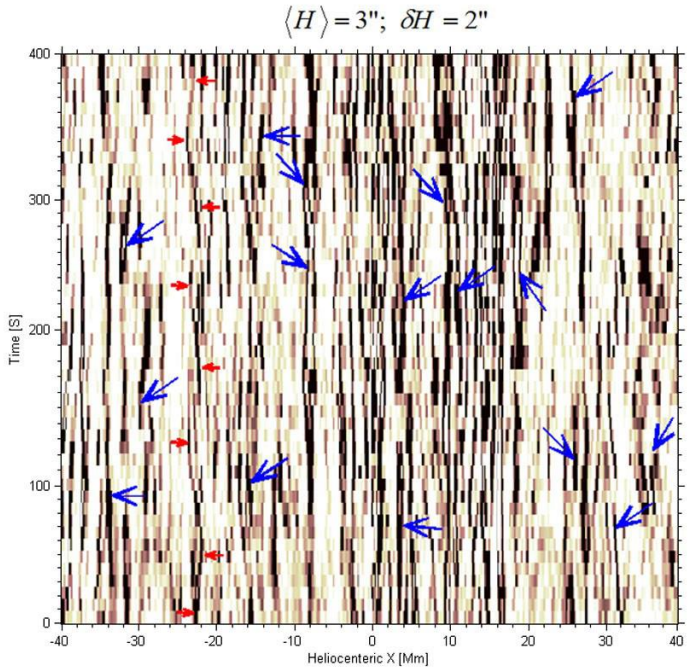

Figure 11: Sample of time slice image at the 3 arcsec height above the limb. In order to improve the time slice result and reduce the noise, an average intensity along the y-axis direction taken over a 2 arcsec (20 pixels) interval is shown. The red arrows show a repetitive transverse motion strongly suggesting a twisting or a rotation of a doublet spicule. The doublet threads (spicules) are indicated using blue larger arrows [24].

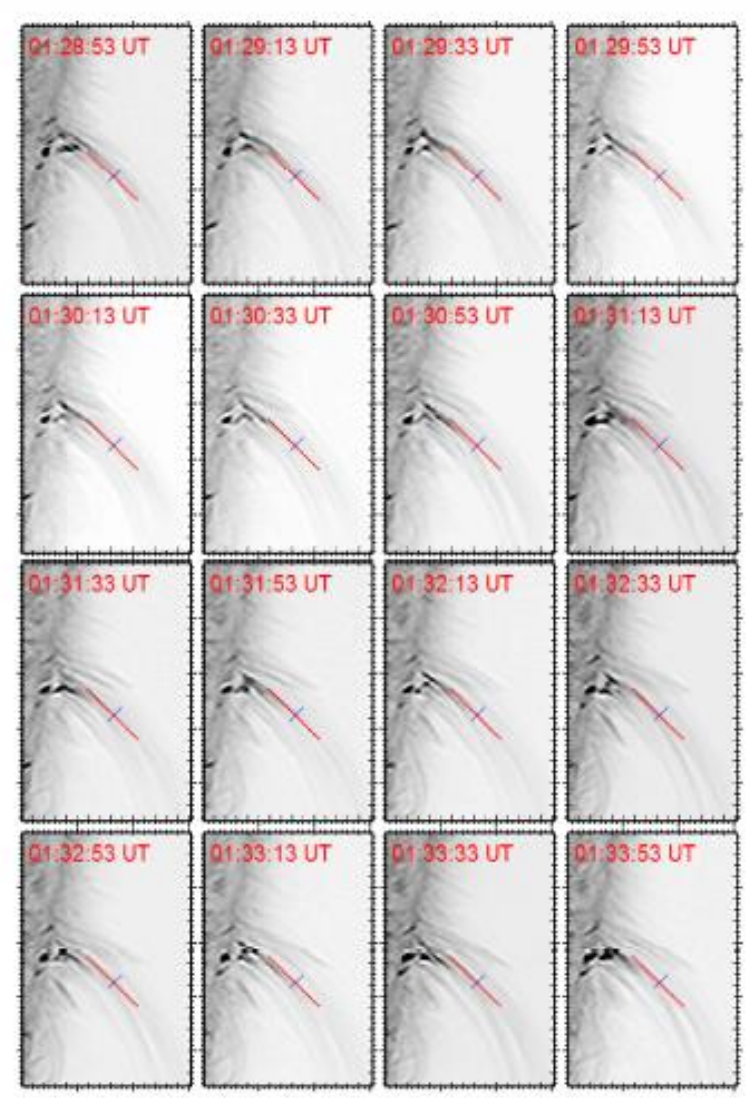

Figure 12: Selected snapshots of negative and mad-maxed images from the SOT (Hinode) broadband Ca II H filter observations (1525 arcsec2 FOV) at different times (01:28 to 01:33 UT). Tick marks show .5 arcsec. The spine axis (taking into account all components) are denoted by a dashed red line. The blue line shown in all images and well above the reconnection site position, outlines the location where oscillatory transverse motions and displacement of the most central part are observed, see results in Figure 10 [26].

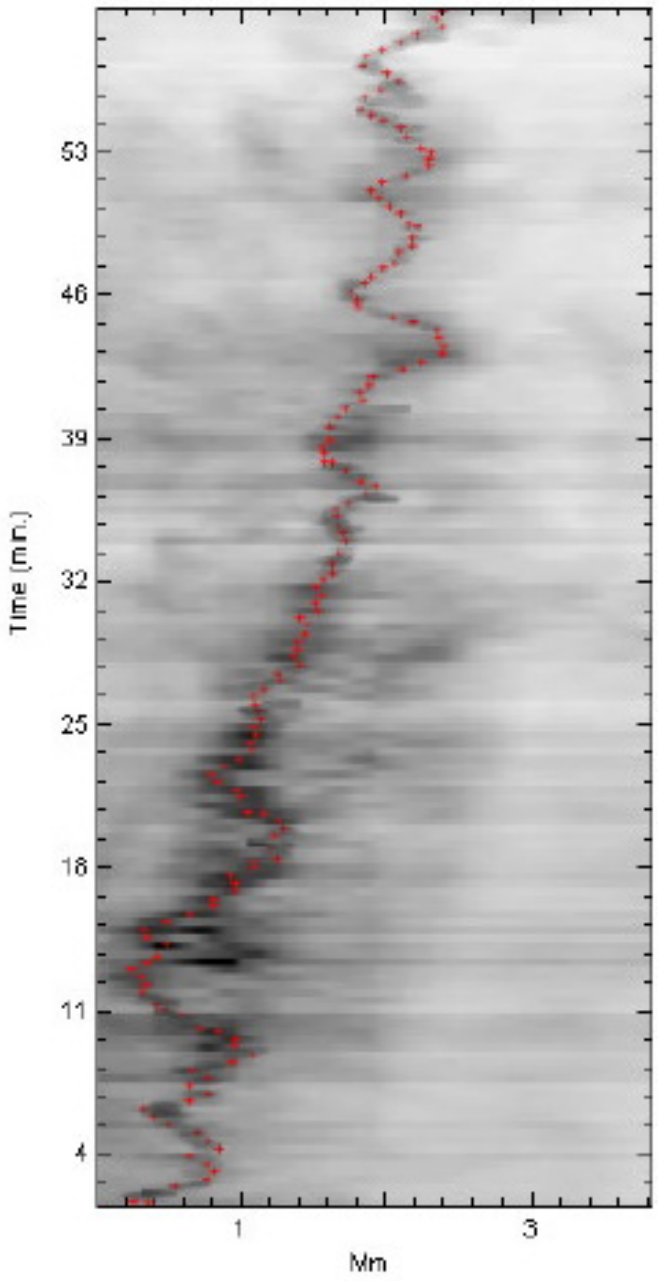

Figure 13: Oscillations in Time slice diagram using real images in taken in the cool Ca II line, using SOT/Hinode observations [26].

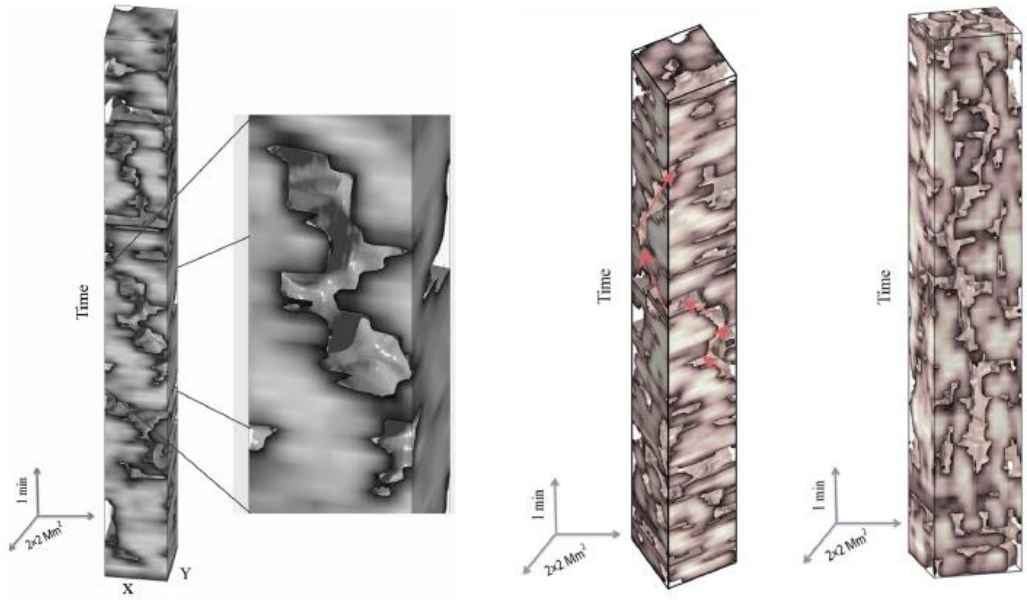

Figure 14: Left: 3D column map shows a vortex velocity of order of 20 km s1 Figure 11. Right :Two different cases for different places and shows long lifetime of rotational behavior [34].

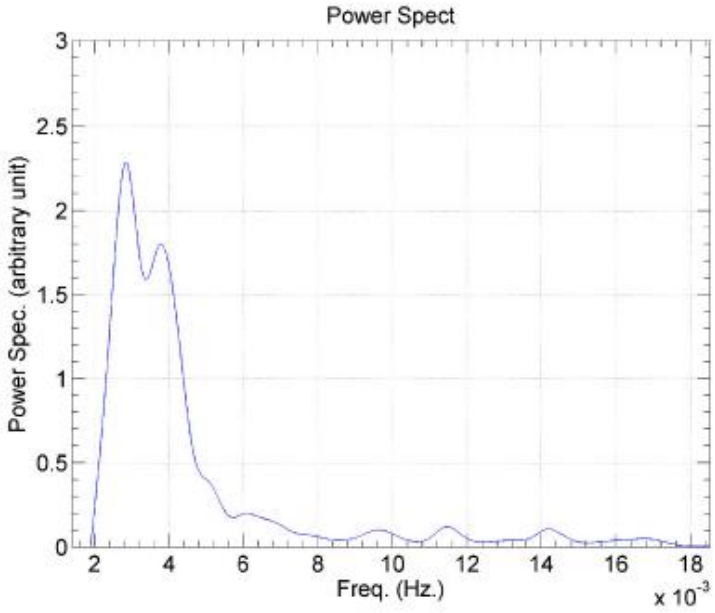

Figure 15: The power spectrum for a region near the center of the Sun for inter network cell without influence of mottles and network bright points intensity fluctuation effect [25].

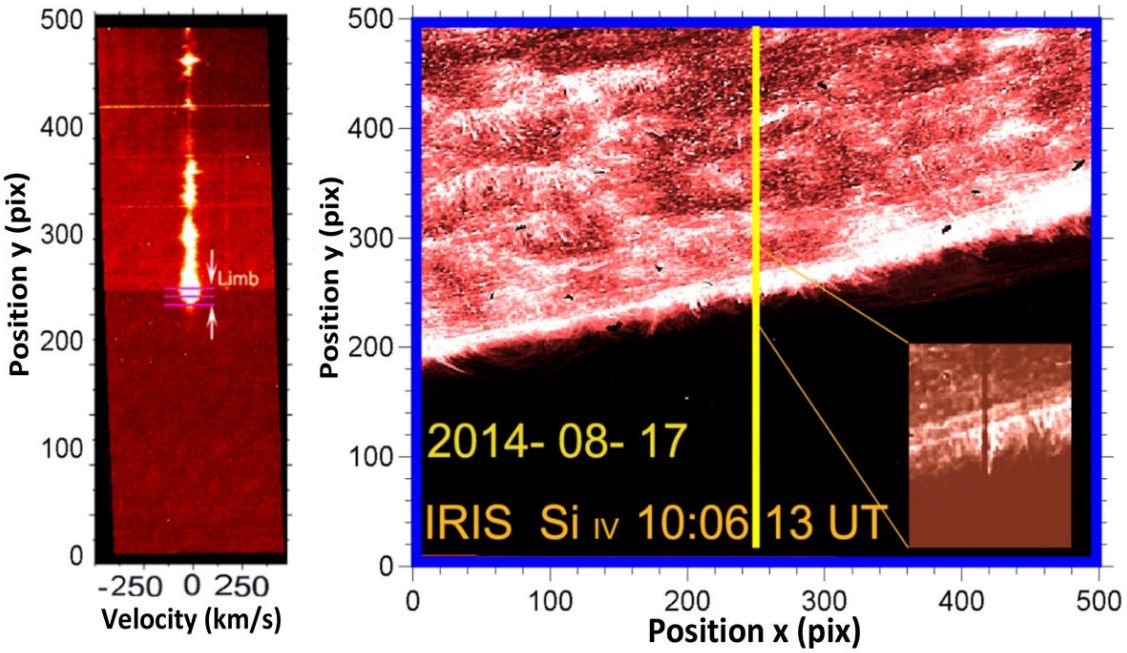

Figure 16: Right: an SJI image recorded by IRIS on August 17th, 2014 at 10:06:13 UT, the yellow line shows the location of the telescope slit, and the bottom image of the side corner on the right is the processed image of the area that points to the studied spicules. Left: an example of the spectrum obtained from the IRIS along the yellow slit at a wavelength of 1400 Å , the three purple horizontal lines show the altitudes under study, the distance between successive altitudes is 2100 km. In these images, each pixel is equivalent to 0.33 arcseconds [43].

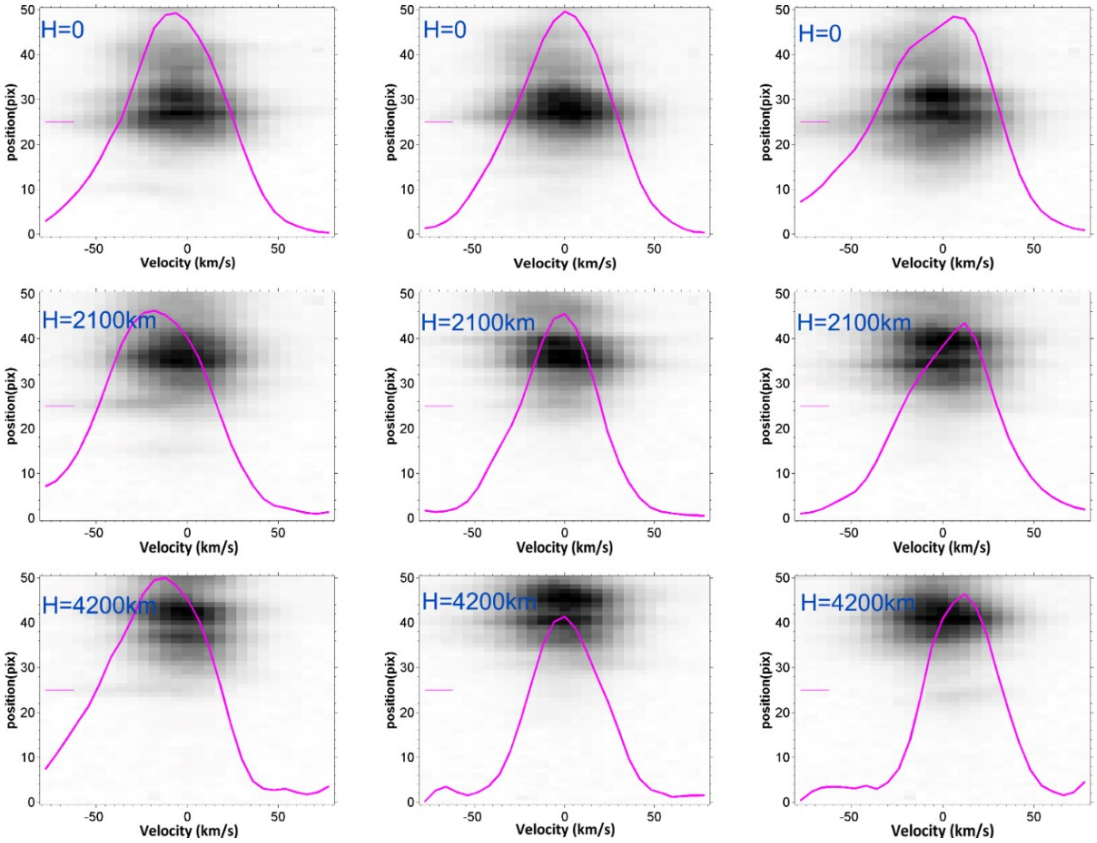

Figure 17: From top to bottom, it shows examples of profile curves obtained at three heights specified in Figure (2b). The first height corresponds to the edge of the sun and the next two heights are considered to be approximately 2100 km apart. Images from right to left show red to blue shifts. The short purple line on the left side of the images indicates the height at which the profiles were obtained [43].

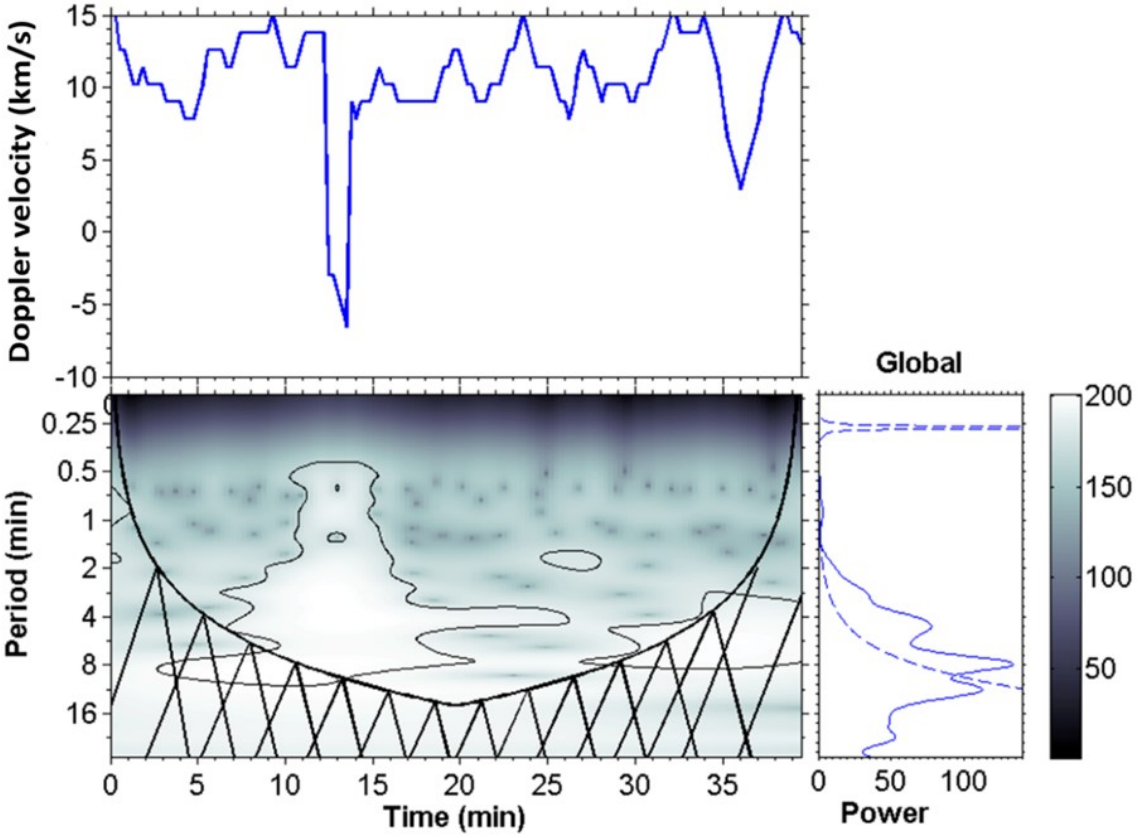

Figure 18: Example of wavelet analysis results of spectrum fluctuations for the first height that is near the edge of the sun. The top figure is the Doppler velocity fluctuations with respect to time, and the bottom figure is the wavelet analysis of these fluctuations in a 40-minute. Fluctuations of 5 and 8-minutes and even a little 3-minute fluctuations are dominant. The hatched area on the figure is the area where the wavelet power spectrum is disturbed due to the effect of the endpoints of the finite length signals [43].

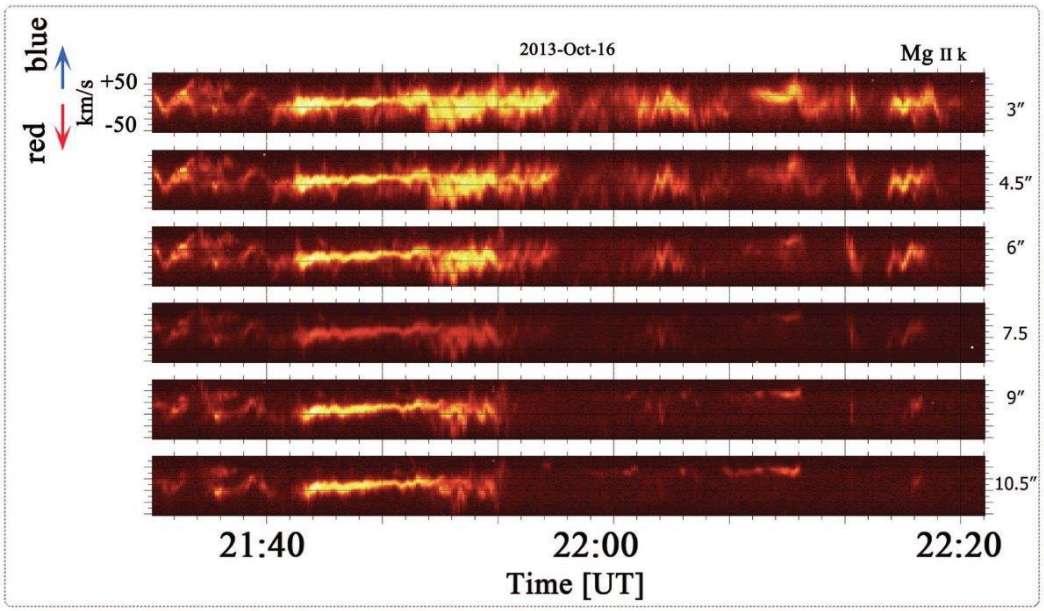

Figure 19: Time sequence of d-spectra in Mg II k line of Oct. 16, 2013 in adjacent layers above the limb on the quiet Sun region at equator. The height difference between each plot is 1.5 arcsec. Waves with periods near 100 sec are well detected near 21:52 to 21:56 UT [32].

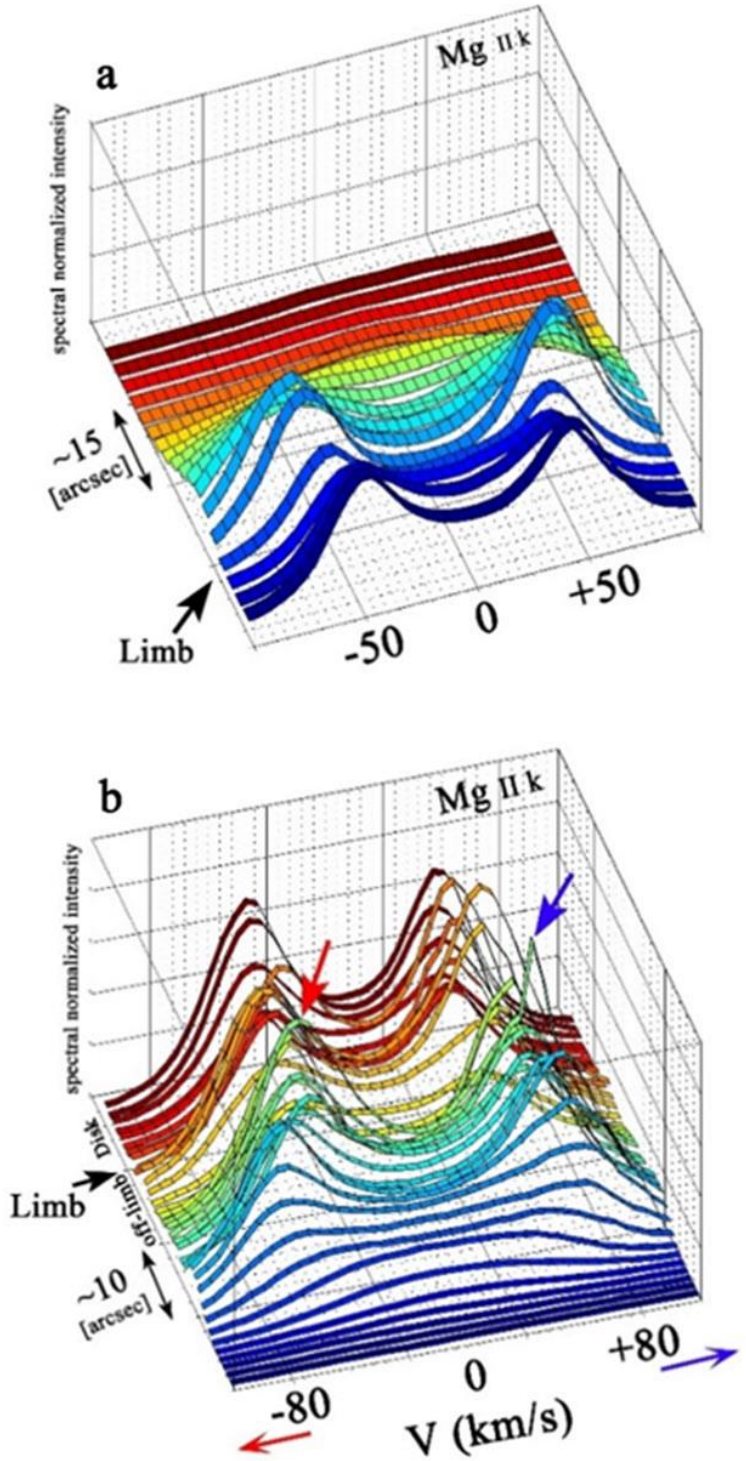

Figure 20: Top and bottom panels are the line profiles of Mg II k 2796 spectra plotted as a function of velocity recorded on 17 August and 19 February 2014, respectively [36].